PHYSICAL REVIEW E VOLUME 52, NUMBER 5 NOVEMBER 1995

Derivation of the inertial ac response for the Kerr-effect relaxation from the Langevin equation in three-dimensional space

J.-L. Déjardin
Centre d'Etudes Fondamentales, Université de Perpignan, 52 Avenue de Villeneuve, 66860 Perpignan Cedex, France

(Received 15 May 1995)

The Kerr-effect response of an assembly of noninteracting dipolar and anisotropically polarizable spherical molecules is calculated from the Euler-Langevin stochastic differential equations. The solution is obtained using combinations of the Legendre polynomials and the associated Legendre functions as angular variables, together with the Hermite polynomials as angular velocity variables. The molecules are compelled to rotate in three-dimensional space and are acted on by a dc bias field, superimposed on which is an ac electric field in the same direction. When the response is restricted to second order in the applied field, the coupling of the fields gives rise to two distinct nonlinear harmonic components of the complex birefringence, varying at the fundamental (ω) and the second harmonic (2ω) of the ac field. Small inertial effects are considered, and their importance is illustrated in numerous dispersion and Cole-Cole plots for various values of the parameter P measuring the balance between induced and permanent dipole moments and a fixed value of the inertial parameter γ. Special emphasis is placed on the phase angles between in-phase and out-of-phase harmonic terms whose values may be multiplied by a factor of 2 at high frequencies, compared to those obtained in the rotational diffusion limit (Debye's model), thus allowing possible practical applications. The transition matrix that is appropriate to dielectric relaxation is also given, since a knowledge of it in the nonlinear case, unlike the aftereffect solution, is needed for the description of the dynamic Kerr effect.

PACS number(s): 05.40.+j, 78.20.Fm, 77.22.Gm

I. INTRODUCTION

In recent years, considerable efforts have been made in the study of electro-optical relaxation phenomena, e.g., dielectric [1,2], Kerr-effect [3–7], and magnetic relaxation [8], for the purpose of obtaining satisfactory calculations of inertial effects on the rotational Brownian motion of molecules in a liquid. When these effects are ignored, the relevant equation that governs the evolution of the orientational distribution function is the Smoluchowski equation written in configuration space. As is well known, the rotational diffusion model initially proposed by Debye [9] leads to a dielectric absorption spectrum without returning to transparency at high frequencies and indeed holds only at low angular frequencies such that $\omega < \tau_1^{-1}$, τ_1 being the dielectric relaxation time. Thus a suitable approach to inertial effects requires one to work in configuration angular velocity space. This may be made either from the Fokker-Planck-Kramers (FPK) equation for the probability density function or from an averaging procedure of the nonlinear Euler-Langevin equations. Both methods have been previously used to calculate the aftereffect solution (following the sudden removal of a constant external electric field) for the Kerr effect relaxation of an assembly of three-dimensional (3D) needlelike rotators: the first method has been used by Kalmykov and Quinn [6], who have considered polar and anisotropically polarizable molecules; using the second method, Coffey *et al.* [7] have calculated the Kerr-effect response of noninteracting dipolar molecules only. Experimental investigations on the femtosecond optical Kerr effect in nitrobenzene and chlorobenzene have shown the necessity for the inclusion of molecular inertia for explaining the full temporal profiles [10]. Thus an inertial theory must be used in view of an adequate description of the ac Kerr response at very high frequencies. It is this aspect we shall develop in the present paper for spherical molecules (or symmetric tops) having both permanent and dipole induced moments and subjected to the action of a dc electric field superimposed on an ac electric field. Moreover, we shall restrict that response up to terms of the squared field only. Also, we must bear into mind that the birefringence arising from the presence of permanent dipole moments is, in essence, nonlinear in such a way that the aftereffect solution for the Kerr-effect relaxation, unlike the linear dielectric response, cannot be used to obtain the ac Kerr-effect response.

In a previous paper [4], we solved the FPK equation for the orientation of a molecule rotating in a plane (disk model) and acted on by a dc bias field superimposed on an ac field. We then derived analytic expressions for the steady-state birefringence in the form of complex birefringence functions leading to harmonic components. Our objective here is to extend these results for rotation in three dimensions corresponding to a more realistic physical model in order to compare them to those obtained with zero inertia in earlier work [11]. However, we shall not consider as a starting equation the FPK equation insofar as this equation leads to calculations that become rapidly much more tedious in 3D than in 2D space. We shall rather illustrate our procedure by using the Euler-Langevin stochastic differential equations [1].

II. THE KERR-EFFECT EQUATION FOR THE ROTATING SPHERE MODEL

We consider a dielectric liquid consisting of an assembly of rigid noninteracting spherical molecules acted on by an electric field of the form $E(t)=E_c+E_0\cos(\omega t)$, that is, a constant bias field on which an ac field is superimposed in the same direction. Since any collective effect is neglected, we may state that this assembly pertains to a closed system undergoing independent rotational motions. This allows one to reduce the problem to the orientational motion of an individual molecule, which may be described from the Euler angles $\vartheta(t),\varphi(t),\psi(t)$ as shown in Fig. 1. We now assume that this molecule carries a permanent (field-off) dipole moment μ situated at its center. The dipole axis is directed along one diameter (the Ox_3 axis) and makes an angle ϑ with the field direction (OZ) at time t. We also assume that the molecule is anisotropically polarizable so that the total dipole moment is

$$\mathbf{m}=\boldsymbol{\mu}+\boldsymbol{\alpha}\mathbf{E}\ , \tag{1}$$

where $\boldsymbol{\alpha}$ is the two-by-two molecular polarizability tensor. The orientational torque produced by $E(t)$ is therefore given by

$$\mathbf{T}=\mathbf{m}\times\mathbf{E}\ . \tag{2}$$

If the geometric axes of the molecule are chosen to be coincident with those of the polarizability tensor, the magnitude of the torque T may be expressed as

$$T=-\mu E\sin\vartheta-(\alpha_{\parallel}-\alpha_{\perp})E^2\sin\vartheta\cos\vartheta\ , \tag{3}$$

where $\alpha_{\parallel}$ and $\alpha_{\perp}$ are the principal electric polarizabilities parallel and perpendicular to the dipole axis ($\alpha_{\parallel}=\alpha_3$ and $\alpha_{\perp}=\alpha_1=\alpha_2$). We then deduce the orientational potential energy

$$\begin{aligned}V&=-\boldsymbol{\mu}\cdot\mathbf{E}-\tfrac{1}{2}\mathbf{E}\boldsymbol{\alpha}\mathbf{E}\ ,\\ &=-\mu E\cos\vartheta-\tfrac{1}{2}\Delta\alpha E^2\cos^2\vartheta-\tfrac{1}{2}\alpha_{\perp}E^2\ ,\end{aligned} \tag{4}$$

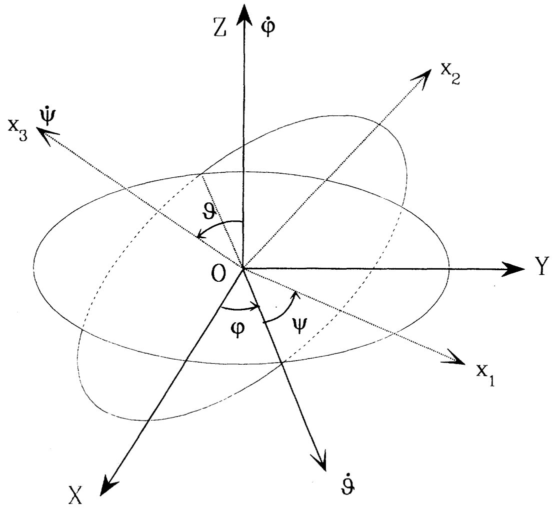

FIG. 1. Definition of Euler angles and associated angular velocities.

where $\Delta\alpha=\alpha_{\parallel}-\alpha_{\perp}$ and

$$\boldsymbol{\alpha}=\begin{bmatrix}\alpha_{\perp}&0&0\\0&\alpha_{\perp}&0\\0&0&\alpha_{\parallel}\end{bmatrix}\ . \tag{5}$$

We denote by I the moment of inertia of the spherical particle about one of its diameters. Hence, following McConnell [1] and using Eq. (3), the Euler-Langevin equations that govern the rotational Brownian motion of the sphere in the presence of the driving field are

$$\begin{aligned}I\frac{d\omega_1}{dt}&=-I[\omega_2(\omega_3-\omega_2\cot\vartheta)]-\mu E(t)\sin\vartheta\\&\quad-\Delta\alpha E^2(t)\sin\vartheta\cos\vartheta-\xi\omega_1+\lambda_1(t)\ ,\end{aligned} \tag{6a}$$

$$I\frac{d\omega_2}{dt}=I[\omega_1(\omega_3-\omega_2\cot\vartheta)]-\xi\omega_2+\lambda_2(t)\ , \tag{6b}$$

$$I\frac{d\omega_3}{dt}=-\xi\omega_3+\lambda_3(t)\ , \tag{6c}$$

where $\boldsymbol{\omega}=(\omega_1,\omega_2,\omega_3)$ is the angular velocity vector, the components of which are (see Fig. 1)

$$\omega_1=\dot\vartheta,\quad \omega_2=\dot\varphi\sin\vartheta,\quad \omega_3=\dot\varphi\cos\vartheta+\dot\psi \tag{7}$$

ξ is the rotational friction coefficient experienced by the molecule in the fluid, so giving rise to a viscous drag torque $-\xi\boldsymbol{\omega}$, and $\boldsymbol{\lambda}(t)=(\lambda_1,\lambda_2,\lambda_3)$ is a random torque (white noise) exerted by the thermal bath (environment) on the molecule. It is generally assumed that the stochastic process associated with the random motion of a Brownian particle is a white noise so that it has the properties

$$\overline{\lambda_i(t)}=\overline{\lambda_j(t)}=0\ , \tag{8a}$$

$$\overline{\lambda_i(0)\lambda_j(t)}=2kT\xi\delta_{ij}\delta(t)\ ,\quad i,j=1,2,3, \tag{8b}$$

where δ_{ij} is the Kronecker symbol, δ is the Dirac delta function, k is the Boltzmann constant, and T is the absolute temperature. The overbars represent the statistical average over a large number of rotators that all started with the same angular velocity (sharp initial condition). In what follows, we shall focus our attention on the first differential equation [Eq. (6a)] insofar as it is the only one that is field dependent. As originally suggested by Frood and Lal [12] and then undertaken by Coffey [3], we rewrite Eq. (6a) by effecting the changes of variables

$$p(t)=\mu P_1(\cos\vartheta)=\mu\cos\vartheta\ , \tag{9a}$$

$$K(t)=\mu^2P_2(\cos\vartheta)=\mu^2(3\cos^2\vartheta-1)/2\ , \tag{9b}$$

where P_1 and P_2 are the first- and second-order Legendre polynomials, the expected values of which are appropriate to dielectric and Kerr effect relaxation, respectively. We then obtain

$$\dot\vartheta(t)=\omega_1(t)=-\frac{\dot K(t)}{3(\mu^2-p^2)^{0.5}p(t)}\ , \tag{10a}$$

$$\ddot\vartheta(t)=\dot\omega_1(t)=-\frac{\ddot K(t)+[4K(t)-\mu^2]\dot\vartheta^2(t)}{3(\mu^2-p^2)^{0.5}p(t)}\ , \tag{10b}$$

so that Eq. (6a) takes the form

$$I\ddot{K}(t)+\xi\dot{K}(t)+I(4\dot{\vartheta}^2+2\omega_2^2)K(t)-3I\omega_2\omega_3(\mu^2-p^2)^{0.5}p(t)$$
$$=I\mu^2(\dot{\vartheta}^2-\omega_2^2)+3(\mu^2-p^2)E(t)p(t)+3\frac{\Delta\alpha}{\mu^2}(\mu^2-p^2)E^2(t)p^2(t)-3(\mu^2-p^2)^{0.5}p(t)\lambda_1(t)\ . \qquad (11)$$

This equation provides us with the time evolution of $K(t)$ and so is characteristic of the Kerr-effect relaxation in the presence of the driving field $E(t)$. It agrees with that of Coffey, who considered the case of polar molecules only ($\Delta\alpha=0$) [3].

At this stage of our investigation, it is interesting to see what happens in the long time limit, that is, for t much larger than τ_F, the friction time equal to I/ξ. This situation occurs in the case of vanishingly small inertia. The components of the angular velocity may therefore be regarded as centered Gaussian stochastic variables, so that [1]

$$\langle\omega_i(0)\omega_j(t)\rangle=\delta_{ij}\frac{kT}{I}\exp(-|t|/\tau_F)\ . \qquad (12)$$

Averaging Eq. (11) over configuration angular velocity space and using Eqs. (8) and (12), we have

$$\xi\langle\dot{K}\rangle+6kT\langle K\rangle$$
$$=\tfrac{6}{5}\mu^3E(t)(\langle P_1\rangle-\langle P_3\rangle$$
$$+3\Delta\alpha\mu^2E^2(t)(\tfrac{2}{21}\langle P_2\rangle-\tfrac{8}{35}\langle P_4\rangle+\tfrac{2}{15})\ , \qquad (13)$$

where P_3 and P_4 denote the Legendre polynomials of order 3 and 4, respectively, arising from the calculations of

$$p(\mu^2-p^2)=\mu^3(1-\cos^2\vartheta)\cos\vartheta=\tfrac{2}{5}\mu^3(P_1-P_3)\ , \qquad (14a)$$

$$p^2(\mu^2-p^2)=\mu^4(\cos^2\vartheta-\cos^4\vartheta)$$
$$=\mu^4(\tfrac{2}{15}+\tfrac{2}{21}P_2-\tfrac{8}{35}P_4)\ , \qquad (14b)$$

and, according to the theorem of equipartition of energy,

$$\lim_{I\to 0}\langle I(4\dot{\vartheta}^2+2\omega_2^2)K\rangle=6kT\langle K\rangle\ . \qquad (14c)$$

The angular brackets in Eq. (13) denote a dual average, which may be described as follows (see [13,14]). First, by interpreting the stochastic Euler-Langevin equation (11) as an integral equation and applying the Stratonovitch rule [14], we perform the average (denoted by an overbar) over a set of rotators that all started with the same (sharp initial conditions) angular velocity. This procedure [13,14] allows us to represent the problem of calculating the desired average [in this case $P_2(\cos\vartheta)$] as that of solving a set of deterministic equations governing the time evolution of the set of sharp starting values (in the FPK equation approach the procedure generates the set of differential-recurrence relations governing the time evolution of the *transition probability,* which requires a δ function, i.e., a *sharp* initial distribution). Next we suppose instead of the sharp value a Maxwellian distribution (thermal equilibrium) for the initial values of the angular velocities in this set; the average with this distribution is denoted by $\langle\ \rangle$, the overbar denoting the first average being deleted for economy of notation. Dividing across both sides of Eq. (13) by $\mu^2\xi$, we have

$$\frac{1}{D}\langle\dot{P}_2\rangle+6\langle P_2\rangle=\tfrac{6}{5}\Gamma(t)(\langle P_1\rangle-\langle P_3\rangle)$$
$$+B(t)(\tfrac{2}{7}\langle P_2\rangle-\tfrac{24}{35}\langle P_4\rangle+\tfrac{2}{5})\ , \qquad (15)$$

where D is the rotational diffusion constant equal to kT/ξ and

$$\Gamma(t)=\frac{\mu}{kT}E(t)\ ,\quad B(t)=\frac{\Delta\alpha}{kT}E^2(t)\ . \qquad (16)$$

Equation (15) is a differential-recurrence relation that coincides exactly for $n=2$ with that obtained by solution of the Smoluchowski equation, namely [15],

$$\frac{1}{D}\langle\dot{P}_n\rangle+n(n+1)\langle P_n\rangle=\Gamma(t)\frac{n(n+1)}{2n+1}(\langle P_{n-1}\rangle-\langle P_{n+1}\rangle)$$
$$+B(t)\left[\frac{n(n+1)}{(2n-1)(2n+3)}\langle P_n\rangle+\frac{(n-1)n(n+1)}{(2n-1)(2n+1)}\langle P_{n-2}\rangle-\frac{n(n+1)(n+2)}{(2n+1)(2n+3)}\langle P_{n+2}\rangle\right]\ . \qquad (17)$$

III. MATRIX FORMULATION OF THE DYNAMIC KERR-EFFECT RESPONSE

When inertial effects are taken into account, the angular velocities can no longer be considered as in thermal equilibrium. This means that the velocity distribution function does not follow a Maxwell-Boltzmann law. Taking the ensemble average over each term of Eq. (11) and noting that

$$\langle(\mu^2-p^2)^{0.5}p(t)\lambda_1(t)\rangle=\langle(\mu^2-p^2)^{0.5}p(t)\rangle\langle\lambda_1(t)\rangle=0\ , \qquad (18)$$

this equation becomes

$$\langle \ddot{K} \rangle + \beta \langle \dot{K} \rangle + 2\alpha^2 \langle K[H_2(\Omega_1) + \tfrac{1}{2}H_2(\Omega_2) + 3] \rangle - \frac{\alpha^2\mu^2}{2} \langle P_2^1 H_1(\Omega_2) H_1(\Omega_3) \rangle$$
$$= \frac{\alpha^2\mu^2}{2} \langle [H_2(\Omega_1) - H_2(\Omega_2)] \rangle + \frac{6}{5}\frac{\mu^3 E}{I} \langle P_1 - P_3 \rangle + 3\frac{\Delta\alpha}{I}\mu^2 E^2 \langle \tfrac{2}{15} + \tfrac{2}{21}P_2 - \tfrac{8}{35}P_4 \rangle \,, \quad (19a)$$

or in terms of the second Legendre polynomial

$$\langle \ddot{P}_2 \rangle + \beta \langle \dot{P}_2 \rangle + 2\alpha^2 \langle P_2[H_2(\Omega_1) + \tfrac{1}{2}H_2(\Omega_2) + 3] \rangle - \frac{\alpha^2}{2} \langle P_2^1 H_1(\Omega_2) H_1(\Omega_3) \rangle$$
$$= \frac{\alpha^2}{2} \langle [H_2(\Omega_1) - H_2(\Omega_2)] \rangle + \frac{6}{5}\frac{\mu E}{I} \langle P_1 - P_3 \rangle + 3\frac{\Delta\alpha}{I} E^2 \langle \tfrac{2}{15} + \tfrac{2}{21}P_2 - \tfrac{8}{35}P_4 \rangle \,, \quad (19b)$$

where

$$\beta = 1/\tau_F = \xi/I \,, \quad \alpha^2 = kT/I \,, \quad \omega_i = \alpha\sqrt{2}\Omega_i \quad (i = 1,2,3) \,,$$

$H_2(\Omega_i) = 4\Omega_i^2 - 2$ is the Hermite polynomial of order 2 associated with the angular velocities, and $P_2^1(u = \cos\vartheta)$ is the associated Legendre function of second order such that

$$P_k^m(u) = \sqrt{(1-u^2)^m} \frac{d^m}{du^m} P_k(u) \,.$$

From Eq. (9b), we have

$$\langle \dot{P}_2 \rangle = -\langle (3 \sin\vartheta \cos\vartheta)\dot{\vartheta} \rangle$$
$$= -\langle P_2^1 \alpha\sqrt{2}\Omega_1 \rangle$$
$$= -\frac{\alpha\sqrt{2}}{2} \langle P_2^1 H_1(\Omega_1) \rangle = -\frac{\alpha\sqrt{2}}{2} \langle Z_1 \rangle \,, \quad (20)$$

where $H_1(\Omega_1) = 2\Omega_1$ is the first Hermite polynomial and hence Eq. (19b) reduces to

$$\frac{d}{dt} \langle Z_1 \rangle + \beta \langle Z_1 \rangle$$
$$= \alpha\sqrt{2} \langle P_2[2H_2(\Omega_1) + H_2(\Omega_2)] - \frac{H_2(\Omega_1) - H_2(\Omega_2)}{2}$$
$$- \frac{1}{2} P_2^1 H_1(\Omega_2) H_1(\Omega_3) \rangle + 6\alpha\sqrt{2} \langle P_2 \rangle$$
$$- \frac{6}{5}\sqrt{2}\frac{\mu E}{I\alpha} \langle P_1 \rangle - \frac{2}{5}\sqrt{2}\frac{\Delta\alpha}{I\alpha} E^2 \quad (21)$$

if we restrict ourselves to the response to second order in the electric field strength (the products $E\langle P_3 \rangle$, $E^2\langle P_2 \rangle$, and $E^2\langle P_4 \rangle$ would be at least of order E^4, E^4, and E^6, respectively). The next differential equation will be given by the time evolution of the leading term on the right-hand side of Eq. (21), namely,

$$\frac{d}{dt} \langle Z_2 \rangle = \langle \dot{Z}_2 \rangle = \frac{d}{dt} \Big\langle P_2[2H_2(\Omega_1) + H_2(\Omega_2)]$$
$$- \frac{H_2(\Omega_1) - H_2(\Omega_2)}{2}$$
$$- \frac{1}{2} P_2^1 H_1(\Omega_2) H_1(\Omega_3) \Big\rangle \,. \quad (22)$$

The details of that calculation are given in Appendix A. We have

$$\langle \dot{Z}_2 \rangle + 2\beta \langle Z_2 \rangle = -\frac{11\alpha\sqrt{2}}{2} \langle Z_1 \rangle - \frac{3\alpha}{\sqrt{2}} \langle (P_2 - 1) H_1(\Omega_1) H_1(\Omega_2) H_1(\Omega_3) \rangle$$
$$- \alpha\sqrt{2} \langle P_2^1 [H_1(\Omega_1) H_2(\Omega_2) + H_3(\Omega_1) + \tfrac{1}{4} H_1(\Omega_1) H_2(\Omega_3)] \rangle - \frac{8\mu E}{5I\alpha\sqrt{2}} \langle (P_3^1 - P_1^1) H_1(\Omega_1) \rangle$$
$$- \frac{8\Delta\alpha}{3I\alpha\sqrt{2}} E^2 \langle (\tfrac{9}{35} P_4^1 - \tfrac{1}{7} P_2^1) H_1(\Omega_1) \rangle + \frac{2\mu E}{I\alpha\sqrt{2}} \langle P_1^1 H_1(\Omega_1) \rangle + \frac{2\Delta\alpha}{3I\alpha\sqrt{2}} E^2 \langle P_2^1 H_1(\Omega_1) \rangle \,. \quad (23)$$

The Kerr-effect response to order E^2 is the quantity of interest, so that terms such as $E\langle P_3^1 H_1(\Omega_1) \rangle$, $E^2\langle P_2^1 H_1(\Omega_1) \rangle$, and $E^2\langle P_4^1 H_1(\Omega_1) \rangle$ may still be neglected. Equation (23) then becomes

$$\langle \dot{Z}_2 \rangle + 2\beta \langle Z_2 \rangle = -\frac{11\alpha\sqrt{2}}{2} \langle Z_1 \rangle - \alpha\sqrt{2} \langle P_2^1 [H_1(\Omega_1) H_2(\Omega_2) + H_3(\Omega_1) + \tfrac{1}{4} H_1(\Omega_1) H_2(\Omega_3)]$$
$$+ \tfrac{3}{2}(P_2 - 1) H_1(\Omega_1) H_1(\Omega_2) H_1(\Omega_3) \rangle + \frac{9\sqrt{2}}{5I\alpha} \mu E \langle z_1 \rangle \,, \quad (24)$$

where

$$\langle z_1 \rangle = \langle P_1^1 H_1(\Omega_1) \rangle \ , \tag{25a}$$

$$\langle Z_3 \rangle = \langle P_2^1 [H_1(\Omega_1)H_2(\Omega_2) + H_3(\Omega_1) + \tfrac{1}{4} H_1(\Omega_1) H_2(\Omega_3)] + \tfrac{3}{2}(P_2 - 1) H_1(\Omega_1) H_1(\Omega_2) H_1(\Omega_3) \rangle \ . \tag{25b}$$

If we stop the procedure at this level, we obtain the 3×3 approximation. Indeed, Eqs. (20), (21), and (24) may be gathered in a matrix form as

$$\begin{bmatrix} \frac{d}{dt}\langle P_2 \rangle \\ \frac{d}{dt}\langle Z_1 \rangle \\ \frac{d}{dt}\langle Z_2 \rangle \end{bmatrix} = \begin{bmatrix} 0 & -\alpha/\sqrt{2} & 0 \\ 6\alpha\sqrt{2} & -\beta & \alpha\sqrt{2} \\ 0 & -\frac{11\alpha}{\sqrt{2}} & -2\beta \end{bmatrix} \begin{bmatrix} \langle P_2 \rangle \\ \langle Z_1 \rangle \\ \langle Z_2 \rangle \end{bmatrix} + \frac{3\sqrt{2}}{5I\alpha}\mu E(t) \begin{bmatrix} 0 \\ -2\langle P_1 \rangle \\ 3\langle z_1 \rangle \end{bmatrix} - \frac{2\sqrt{2}}{5I\alpha}\Delta\alpha E^2(t) \begin{bmatrix} 0 \\ 1 \\ 0 \end{bmatrix} \tag{26a}$$

or

$$[\dot{\mathbf{p}}_2(t)] = [\mathbf{M}_2][\mathbf{p}_2(t)] - \frac{6\sqrt{2}}{5I\alpha}\mu E(t)[\mathbf{C}_1(t)] + \frac{3\sqrt{2}}{5I\alpha}\mu E(t)[\mathbf{D}_1(t)] - \frac{2\sqrt{2}}{5I\alpha}\Delta\alpha E^2(t)[\mathbf{C}_0] \ , \tag{26b}$$

where

$$[\dot{\mathbf{p}}_2(t)] = \begin{bmatrix} \langle \dot{P}_2 \rangle \\ \langle \dot{Z}_1 \rangle \\ \langle \dot{Z}_2 \rangle \end{bmatrix} , \quad [\mathbf{M}_2] = \begin{bmatrix} 0 & -\alpha/\sqrt{2} & 0 \\ 6\alpha\sqrt{2} & -\beta & \alpha\sqrt{2} \\ 0 & -11\alpha/\sqrt{2} & -2\beta \end{bmatrix} , \quad [\mathbf{p}_2(t)] = \begin{bmatrix} \langle P_2 \rangle \\ \langle Z_1 \rangle \\ \langle Z_2 \rangle \end{bmatrix} ,$$
$$[\mathbf{C}_1(t)] = \begin{bmatrix} 0 \\ \langle P_1 \rangle \\ \langle z_1 \rangle \end{bmatrix} , \quad [\mathbf{D}_1(t)] = \begin{bmatrix} 0 \\ 0 \\ \langle z_1 \rangle \end{bmatrix} , \quad [\mathbf{C}_0] = \begin{bmatrix} 0 \\ 1 \\ 0 \end{bmatrix} . \tag{26c}$$

$[\mathbf{M}_2]$ represents the transition matrix, $[\mathbf{C}_1(t)]$, $[\mathbf{D}_1(t)]$, and $[\mathbf{C}_0]$ may be regarded as driving field matrices. In the treatment of the aftereffect Kerr response for polar linear rotators, Coffey *et al.* [7] argued that the 3×3 truncation was not correct because $\langle \dot{Z}_3 \rangle$ contains not only a $\langle Z_2 \rangle$ term but also a $\langle Z_2' \rangle$ term with similar second-order Hermite polynomials. Thus it was concluded that it was necessary to calculate $\langle \dot{Z}_2' \rangle$ and to include it before $\langle \dot{Z}_3 \rangle$, so that the good approximation would be 4×4 and not 3×3. We have verified this (see Appendix A) and found that, in fact, both 3×3 and 4×4 approximations are completely equivalent. This remark is important insofar as it allows us to carry out the calculations from a 3×3 transition matrix, which is much easier to manipulate than a 4×4 one.

IV. SOLUTION BY FOURIER TRANSFORM METHODS

By inspection of Eq. (26a), one sees that the determination of $\langle P_2 \rangle$, $\langle Z_1 \rangle$, and $\langle Z_2 \rangle$ requires that of $\langle P_1 \rangle$ and $\langle z_1 \rangle$, which are characteristic functions of dielectric relaxation. In order to accomplish this, we refer the reader to Appendix B in which a general treatment of the time evolution of the expected value of the nth Legendre polynomial for spherical particles is given. Setting $n = 1$ in Eq. (B7), we have

$$I\langle \ddot{P}_1 \rangle + \xi \langle \dot{P}_1 \rangle + I\langle (\dot{\vartheta}^2 + \omega_2^2) P_1 \rangle = I\langle \omega_2\omega_3 P_1^1 \rangle + \tfrac{2}{3}\mu E(t)\langle 1 - P_2 \rangle + \tfrac{2}{5}\Delta\alpha E^2(t)\langle P_1 - P_3 \rangle \tag{27a}$$

or, if we confine ourselves to second order in the electric field,

$$\langle \ddot{P}_1 \rangle + \beta\langle \dot{P}_1 \rangle + \frac{\alpha^2}{2}\langle P_1[H_2(\Omega_1) + H_2(\Omega_2) + 4] \rangle = \frac{\alpha^2}{2}\langle P_1^1 H_1(\Omega_2) H_1(\Omega_3) \rangle + \frac{2}{3}\frac{\mu E(t)}{I} + \frac{2}{5}\frac{\Delta\alpha E^2(t)}{I}\langle P_1 \rangle \ , \tag{27b}$$

where $P_1^1 = \sin\vartheta$. Further, by definition

$$\langle P_1 \rangle(t) = \langle \cos\vartheta \rangle(t) \ , \tag{28a}$$

so that

$$\langle \dot{P}_1 \rangle = -\langle \dot{\vartheta} \sin\vartheta \rangle = -\frac{\alpha\sqrt{2}}{2}\langle P_1^1 H_1(\Omega_1) \rangle = -\frac{\alpha\sqrt{2}}{2}\langle z_1 \rangle \tag{28b}$$

and Eq. (27b) becomes

$$\frac{d}{dt}\langle z_1 \rangle + \beta\langle z_1 \rangle = 2\alpha\sqrt{2}\langle P_1 \rangle + \frac{\alpha}{\sqrt{2}}\langle z_2 \rangle - \frac{2\sqrt{2}}{3I\alpha}\mu E(t) - \frac{2\sqrt{2}}{5I\alpha}\Delta\alpha E^2(t)\langle P_1 \rangle \ , \tag{29a}$$

where

$$\langle z_2\rangle=\langle P_1[H_2(\Omega_1)+H_2(\Omega_2)]-P_1^1H_1(\Omega_2)H_1(\Omega_3)\rangle \ . \tag{29b}$$

Performing the time derivative of $\langle z_2\rangle$, we find that

$$\begin{aligned}\langle \dot{z}_2\rangle+2\beta\langle z_2\rangle=&-3\alpha\sqrt{2}\langle z_1\rangle-\frac{\alpha}{\sqrt{2}}\langle z_3\rangle\\ &-\frac{4\mu E(t)}{3I\alpha\sqrt{2}}\langle P_2^1H_1(\Omega_1)\rangle\\ &-\frac{4\Delta\alpha}{15I\alpha\sqrt{2}}E^2(t)\\ &\times\langle(2P_3^1+3P_1^1)H_1(\Omega_1)\rangle \ .\end{aligned} \tag{30}$$

The field-dependent terms in Eq. (30) are at least of order E^3 and E^5 and so they may be ignored. From Eqs. (28b), (29a), and (30), the transition matrix for dielectric relaxation of spherical molecules is

$$[\mathbf{M}_1]=\begin{bmatrix}0 & -\alpha/\sqrt{2} & 0\\ 2\alpha\sqrt{2} & -\beta & \alpha/\sqrt{2}\\ 0 & -3\alpha\sqrt{2} & -2\beta\end{bmatrix} , \tag{31}$$

so that the set of these differential equations may be written as

$$[\dot{\mathbf{p}}_1(t)]=[\mathbf{M}_1][\mathbf{p}_1(t)]-\frac{2\sqrt{2}}{3I\alpha}\mu E(t)[\mathbf{C}_0] , \tag{32a}$$

where $[\dot{\mathbf{p}}_1(t)]$ and $[\mathbf{p}_1(t)]$ are column matrices

$$[\dot{\mathbf{p}}_1(t)]=\begin{bmatrix}\langle \dot{P}_1\rangle\\ \langle \dot{z}_1\rangle\\ \langle \dot{z}_2\rangle\end{bmatrix} , \quad [\mathbf{p}_1(t)]=\begin{bmatrix}\langle P_1\rangle\\ \langle z_1\rangle\\ \langle z_2\rangle\end{bmatrix} . \tag{32b}$$

Taking the Fourier transform of both sides of Eq. (32a) yields

$$\begin{aligned}[\mathbf{P}_1(\Omega)]=&-\{i\Omega[\mathbf{I}]-[\mathbf{M}_1]\}^{-1}[\mathbf{C}_0]\\ &\times\{2\pi\lambda_c\delta(\Omega)+\pi\lambda_0[\delta(\omega-\Omega)+\delta(\omega+\Omega)]\} ,\end{aligned} \tag{33}$$

where

$$E(t)=E_c+E_0\cos(\omega t) ,$$

$$\lambda_0=\frac{2\sqrt{2}}{3I\alpha}\mu E_0 , \quad \lambda_c=\frac{2\sqrt{2}}{3I\alpha}\mu E_c , \tag{34a}$$

$$[\mathbf{P}_1(\Omega)]=\int_{-\infty}^{+\infty}[\mathbf{p}_1(t)]\exp(-i\Omega t)dt , \tag{34b}$$

$[\mathbf{I}]$ is the unit matrix, and δ the Dirac distribution. We can proceed in a manner similar to that used to get Eq. (26b) on Fourier transforming this equation, which gives

$$\begin{aligned}[\mathbf{P}_2(\Omega)]=\{i\Omega[\mathbf{i}]-[\mathbf{M}_2]\}^{-1}(&-\tfrac{9}{5}\lambda_c[\mathbf{C}_1(\Omega)]-\tfrac{9}{10}\lambda_0\{[\mathbf{E}][\mathbf{P}_1(\Omega-\omega)]+[\mathbf{E}][\mathbf{P}_1(\Omega+\omega)]\}\\ &+\tfrac{9}{2}\lambda_c[\mathbf{D}_1(\Omega)]+\tfrac{9}{4}\lambda_0\{[\mathbf{H}][\mathbf{P}_1(\Omega-\omega)]+[\mathbf{H}][\mathbf{P}_1(\Omega+\omega)]\}\\ &-[\mathbf{C}_0]\{\beta_E2\pi\delta(\Omega)+\tfrac{1}{2}\beta_0\pi[\delta(2\omega-\Omega)+\delta(2\omega+\Omega)]+2\beta_{0c}\pi[\delta(\omega-\Omega)+\delta(\omega+\Omega)]\}) ,\end{aligned} \tag{35}$$

where $[\mathbf{C}_1(\Omega)]$ and $[\mathbf{D}_1(\Omega)]$ are the Fourier transforms of $[\mathbf{C}_1(t)]$ and $[\mathbf{D}_1(t)]$,

$$\beta_0=\frac{2\sqrt{2}\Delta\alpha}{5I\alpha}E_0^2 , \quad \beta_{0c}=\frac{2\sqrt{2}\Delta\alpha}{5I\alpha}E_cE_0 , \quad \beta_E=\frac{2\sqrt{2}}{5I\alpha}(E_c^2+\tfrac{1}{2}E_0^2) , \tag{36a}$$

and $[\mathbf{E}]$ and $[\mathbf{H}]$ are useful skewed diagonal matrices

$$[\mathbf{E}]=\begin{bmatrix}0&0&0\\1&0&0\\0&1&0\end{bmatrix} , \quad [\mathbf{H}]=\begin{bmatrix}0&0&0\\0&0&0\\0&1&0\end{bmatrix} . \tag{36b}$$

$[\mathbf{P}_1(\Omega\pm\omega)]$ may be evaluated from Eq. (33) by substituting Ω into $\Omega\pm\omega$. Thus the Fourier transform of the Kerr column matrix is

$$
\begin{aligned}
[\mathbf{P}_2(\Omega)]=\{i\Omega[\mathbf{I}]-[\mathbf{M}_2]\}^{-1}\Big(&-\tfrac{9}{5}\lambda_c[\mathbf{E}][P_1(\Omega)]+\tfrac{9}{10}\lambda_0[\mathbf{E}]\{i(\Omega-\omega)[\mathbf{I}]-[\mathbf{M}_1]\}^{-1}\\
&\times[\mathbf{C}_0]\{2\pi\lambda_c\delta(\Omega-\omega)+\pi\lambda_0[\delta(2\omega-\Omega)+\delta(\Omega)]\}+\tfrac{9}{10}\lambda_0[\mathbf{E}]\{i(\Omega+\omega)[\mathbf{I}]-[\mathbf{M}_1]\}^{-1}\\
&\times[\mathbf{C}_0]\{2\pi\lambda_c\delta(\Omega+\omega)+\pi\lambda_0[\delta(2\omega+\Omega)+\delta(\Omega)]\}\\
&+\tfrac{9}{2}\lambda_c[\mathbf{H}][\mathbf{P}_1(\Omega)]-\tfrac{9}{4}\lambda_0[\mathbf{H}]\{i(\Omega-\omega)[\mathbf{I}]-[\mathbf{M}_1]\}^{-1}\\
&\times[\mathbf{C}_0]\{2\pi\lambda_c\delta(\Omega-\omega)+\pi\lambda_0[\delta(2\omega-\Omega)+\delta(\Omega)]\}-\tfrac{9}{4}\lambda_0[\mathbf{H}]\{i(\Omega+\omega)[\mathbf{I}]-[\mathbf{M}_1]\}^{-1}\\
&\times[\mathbf{C}_0]\{2\pi\lambda_c\delta(\Omega+\omega)+\pi\lambda_0[\delta(2\omega+\Omega)+\delta(\Omega)]\}\\
&-[\mathbf{C}_0]\{\beta_E 2\pi\delta(\Omega)+\tfrac{1}{2}\beta_0\pi[\delta(2\omega-\Omega)+\delta(2\omega+\Omega)]+2\beta_{0c}\pi[\delta(\omega-\Omega)+\delta(\omega+\Omega)]\}\Big)\ . \qquad (37)
\end{aligned}
$$

This equation clearly shows that the Kerr-effect response obtained after inversion into time domain consists of two distinct harmonic components varying at the fundamental frequency (ω) and twice the circular frequency (2ω) of the ac field. We also note the presence of time-independent terms, which may be divided into two parts: one is frequency independent and corresponds to terms proportional to λ_c^2 and β_E, while the other is frequency dependent and arises from the permanent dipole moment of the molecule (terms proportional to λ_0^2). The existence of first harmonic terms in ω arising from a coupling effect between dc and ac fields demonstrates a nonlinear behavior of the Kerr response. In addition to this, we must mention that the 2ω response resulting from field-off dipolar moments is nonlinear as well when restricted to second order in E^2.

After many algebraic manipulations checked on a computer in order to avoid errors, the inverse Fourier transform applied to Eq. (37) yields

$$
\begin{aligned}
[\mathbf{p}_2(t)]=&\tfrac{9}{5}\lambda_c^2[\mathbf{M}_2]^{-1}[\mathbf{E}][\mathbf{M}_1]^{-1}[\mathbf{C}_0]-\tfrac{9}{2}\lambda_c^2[\mathbf{M}_2]^{-1}[\mathbf{H}][\mathbf{M}_1]^{-1}[\mathbf{C}_0]+\beta_E[\mathbf{M}_2]^{-1}[\mathbf{C}_0]\\
&-\tfrac{9}{10}\lambda_0^2\mathrm{Re}([\mathbf{M}_2]^{-1}[\mathbf{E}]\{i\omega[\mathbf{I}]-[\mathbf{M}_1]\}^{-1}[\mathbf{C}_0])-\tfrac{9}{4}\lambda_0^2\mathrm{Re}([\mathbf{M}_2]^{-1}[\mathbf{H}]\{i\omega[\mathbf{I}]-[\mathbf{M}_1]\}^{-1}[C_0])\\
&+\tfrac{9}{10}\lambda_0^2\mathrm{Re}(\{i2\omega[\mathbf{I}]-[\mathbf{M}_2]\}^{-1}[\mathbf{E}]\{i\omega[\mathbf{I}]-[\mathbf{M}_1]\}^{-1}[\mathbf{C}_0]\exp(2i\omega t))\\
&-\tfrac{9}{4}\lambda_0^2\mathrm{Re}(\{i2\omega[\mathbf{I}]-[\mathbf{M}_2]\}^{-1}[\mathbf{H}]\{i\omega[\mathbf{I}]-[\mathbf{M}_1]\}^{-1}[\mathbf{C}_0]\exp(2i\omega t))\\
&-\frac{\beta_0}{2}\mathrm{Re}(\{i2\omega[\mathbf{I}]-[\mathbf{M}_2]\}^{-1}[\mathbf{C}_0]\exp(2i\omega t))\\
&+\tfrac{9}{5}\lambda_0\lambda_c\mathrm{Re}(\{i\omega[\mathbf{I}]-[\mathbf{M}_2]\}^{-1}[\mathbf{E}]\{i\omega[\mathbf{I}]-[\mathbf{M}_1]\}^{-1}[\mathbf{C}_0]\exp(i\omega t))\\
&-\tfrac{9}{2}\lambda_0\lambda_c\mathrm{Re}(\{i\omega[\mathbf{I}]-[\mathbf{M}_2]\}^{-1}[\mathbf{H}]\{i\omega[\mathbf{I}]-[\mathbf{M}_1]\}^{-1}[\mathbf{C}_0]\exp(i\omega t))\\
&-\tfrac{9}{5}\lambda_0\lambda_c\mathrm{Re}(\{i\omega[\mathbf{I}]-[\mathbf{M}_2]\}^{-1}[\mathbf{E}][\mathbf{M}_1]^{-1}[\mathbf{C}_0]\exp(i\omega t))\\
&+\tfrac{9}{2}\lambda_0\lambda_c\mathrm{Re}(\{i\omega[\mathbf{I}]-[\mathbf{M}_2]\}^{-1}[\mathbf{H}][\mathbf{M}_1]^{-1}[\mathbf{C}_0]\exp(i\omega t))\\
&-2\beta_{0c}\mathrm{Re}(\{i\omega[\mathbf{I}]-[\mathbf{M}_2]\}^{-1}[\mathbf{C}_0]\exp(i\omega t))\ , \qquad (38)
\end{aligned}
$$

where Re stands for the "real part of." It should be noted that the second and the 12th term in Eq. (38) give zero contributions. Moreover, the only term that is needed in the calculation of $[\mathbf{p}_2(t)]$ is the first element of that column matrix, that is $\langle P_2\rangle(t)$. It is found that

$$
\langle P_2\rangle(t)=\langle P_2\rangle_{\mathrm{st}}(\omega)+\sum_{j=1}^{2}[\Delta n_j'(\omega)\cos(j\omega t)+\Delta n_j''(\omega)\sin(j\omega t)]\ , \qquad (39)
$$

where

$$
\langle P_2\rangle_{\mathrm{st}}(\omega)=\frac{1}{15}\left[\frac{\mu E_c}{kT}\right]^2+\frac{1}{15}\frac{\Delta\alpha}{kT}\overline{E}^2+\frac{1}{15}\frac{\mu^2E_0^2}{I^2\alpha^2}\frac{-\frac{9}{2}\omega^4-2\omega^2(8\alpha^2+9\beta^2)+8\alpha^2\beta^2}{\beta^2(-3\omega^2+4\alpha^2)^2+\omega^2(-\omega^2+2\beta^2+5\alpha^2)^2}\ , \qquad (40a)
$$

the overbar denotes the time average of $E^2(t)$ equal to $E_c^2+0.5E_0^2$, and the subscript st stands for steady state,

$$
\Delta n_2'(\omega)=\frac{2\Delta\alpha}{5I}E_0^2\frac{A\beta+\omega B}{A^2+B^2}+\frac{8\mu^2E_0^2}{5I^2}\frac{(\beta^2-5\omega^2/4)(aA-bB)+3\omega\beta(bA+aB)}{(a^2+b^2)(A^2+B^2)}\ , \qquad (40b)
$$

$$\Delta n_2''(\omega)=\frac{2\Delta\alpha}{5I}E_0^2\frac{\beta B-\omega A}{A^2+B^2}+\frac{8\mu^2E_0^2}{5I^2}\frac{(\beta^2-5\omega^2/4)(bA+aB)-3\omega\beta(aA-bB)}{(a^2+b^2)(A^2+B^2)}\ , \tag{40c}$$

$$\Delta n_1'(\omega)=\frac{1}{5}\left[\frac{\mu^2}{3k^2T^2}+\frac{4\Delta\alpha}{I}\right]E_0E_c\frac{2\beta A'+\omega B'}{A'^2+B'^2}+\frac{8\mu^2}{5I^2}E_0E_c\frac{\mathcal{A}'(-2\omega^2+2\beta^2)+5\omega\beta\mathcal{B}'}{\mathcal{A}'^2+\mathcal{B}'^2}\ , \tag{40d}$$

$$\Delta n_1''(\omega)=\frac{1}{5}\left[\frac{\mu^2}{3k^2T^2}+\frac{4\Delta\alpha}{I}\right]E_0E_c\frac{2\beta B'-\omega A'}{A'^2+B'^2}+\frac{8\mu^2}{5I^2}E_0E_c\frac{\mathcal{B}'(-2\omega^2+2\beta^2)-5\omega\beta\mathcal{A}'}{\mathcal{A}'^2+\mathcal{B}'^2}\ . \tag{40e}$$

a, b, A, B, A', B', $\mathcal{A}'$, and $\mathcal{B}'$ are functions of ω representing the real and imaginary parts that arise from the calculation of the determinants of the 3×3 matrices in Eq. (38). These are defined by

$$\begin{gathered}
\det\{i\omega[\mathbf{I}]-[\mathbf{M}_1]\}=a+ib \quad\text{with } a=\beta(-3\omega^2+4\alpha^2)\ ,\quad b=\omega(-\omega^2+2\beta^2+5\alpha^2)\\
\det\{i2\omega[\mathbf{I}]-[\mathbf{M}_2]\}=A+iB \quad\text{with } A=12\beta(-\omega^2+\alpha^2)\ ,\quad B=\omega(-8\omega^2+4\beta^2+34\alpha^2)\\
\det\{i\omega[\mathbf{I}]-[\mathbf{M}_2]\}=A'+iB' \quad\text{with } A'=3\beta(-\omega^2+4\alpha^2)\ ,\quad B'=\omega(-\omega^2+2\beta^2+17\alpha^2)\\
\det\{i\omega[\mathbf{I}]-[\mathbf{M}_1]\}\ \det\{i\omega[\mathbf{I}]-[\mathbf{M}_2]\}=\mathcal{A}'+i\mathcal{B}'\\
\text{with } \mathcal{A}'=-\omega^6+\omega^4(13\beta^2+22\alpha^2)-\omega^2(92\alpha^2\beta^2+85\alpha^4+4\beta^4)+48\beta^2\alpha^4,\\
\mathcal{B}'=\omega\beta[6\omega^4-\omega^2(82\alpha^2+12\beta^2)+128\alpha^4+32\alpha^2\beta^2]\ .
\end{gathered} \tag{41}$$

With a view toward obtaining expressions for the harmonic components of the birefringence, which may be easier to apply to experiments, we shall now seek to express Eqs. (40a)–(40e) as normalized functions of friction and birefringence relaxation times $\tau_F=I/\xi$ and $\tau=\xi/(6kT)$ and the factor $P=kT(\Delta\alpha/\mu^2)$.

V. NORMALIZED AMPLITUDES FOR THE BIREFRINGENCE FUNCTIONS

Denoting by $X_j(\omega)$ and $Y_j(\omega)$ the real and imaginary parts of the complex birefringence functions normalized to unity, we have

$$X_j(\omega)=\frac{\Delta n_j'(\omega)}{\Delta n_j'(0)}\ ,\quad Y_j(\omega)=\frac{\Delta n_j''(\omega)}{\Delta n_j'(0)}\ , \tag{42}$$

where $\Delta n_j'(0)$ is the value of $\Delta n_j'(\omega)$ at zero frequency,

$$\begin{aligned}X_2(\omega)=\frac{1}{3(P+1)}\Bigg[&\frac{(4-5\omega^2\tau_F^2)A_1+12\omega^2\tau_F\tau B_1}{A_1^2+\omega^2\tau^2B_1^2}\\
&+P\frac{6(1-6\omega^2\tau_F\tau)+\omega^2\tau_F^2(-24\omega^2\tau_F\tau+12\tau/\tau_F+17)}{2(1-6\omega^2\tau_F\tau)^2+(\omega^2\tau_F^2/18)(-24\omega^2\tau_F\tau+12\tau/\tau_F+17)^2}\Bigg]\ ,\end{aligned} \tag{43a}$$

$$\begin{aligned}Y_2(\omega)=\frac{\omega}{3(P+1)}\Bigg[&\frac{(4-5\omega^2\tau_F^2)B_1\tau-12\tau_FA_1}{A_1^2+\omega^2\tau^2B_1^2}\\
&+P\tau_F\frac{12\omega^2\tau_F\tau+12\tau/\tau_F+11}{2(1-6\omega^2\tau_F\tau)^2+(\omega^2\tau_F^2/18)(-24\omega^2\tau_F\tau+12\tau/\tau_F+17)^2}\Bigg]\ ,\end{aligned} \tag{43b}$$

$$\begin{aligned}X_1(\omega)=\frac{1}{P+1}\Bigg[&\frac{1}{3}\frac{(2-2\omega^2\tau_F^2)A_1'+5\omega^2\tau_F\tau B_1'}{A_1'^2+\omega^2\tau^2B_1'^2}\\
&+\left[P+\frac{1}{2}\right]\frac{-\omega^4\tau_F^3\tau+\omega^2\tau_F\tau[-4+(17/6)\tau_F/\tau]+4}{(2-3\omega^2\tau_F\tau)^2+\omega^2\tau_F^2(-\omega^2\tau_F\tau+2\tau/\tau_F+17/6)^2}\Bigg]\ ,\end{aligned} \tag{43c}$$

$$\begin{aligned}Y_1(\omega)=\frac{\omega}{P+1}\Bigg[&\frac{1}{3}\frac{(2-2\omega^2\tau_F^2)\tau B_1'-5\tau_FA_1'}{A_1'^2+\omega^2\tau^2B_1'^2}\\
&+\left[P+\frac{1}{2}\right]\tau_F\frac{\omega^2\tau_F\tau+4\tau/\tau_F+11/3}{(2-3\omega^2\tau_F\tau)^2+\omega^2\tau_F^2(-\omega^2\tau_F\tau+2\tau/\tau_F+17/6)^2}\Bigg]\ ,\end{aligned} \tag{43d}$$

$$\Delta n_2'(0)=\frac{1}{30}\frac{\mu^2E_0^2}{k^2T^2}(P+1)\ , \tag{44a}$$

$$\Delta n'_1(0)=\frac{2}{15}\frac{\mu^2E_0E_c}{k^2T^2}(P+1)\ , \tag{44b}$$

$$A_1=-8\omega^6\tau_F^4\tau^2+\omega^4\tau_F^2\tau^2\left[56+\frac{37}{3}\frac{\tau_F}{\tau}\right]-\omega^2\tau_F^2\left[\frac{85}{18}+\frac{86}{3}\frac{\tau}{\tau_F}+8\frac{\tau^2}{\tau_F^2}\right]+\frac{4}{3}\ , \tag{44c}$$

$$B_1=36\omega^4\tau_F^3\tau-\omega^2\tau_F\tau\left[36+\frac{103}{3}\frac{\tau_F}{\tau}\right]+\frac{4}{3}\left[5+\frac{16}{3}\frac{\tau_F}{\tau}\right]\ , \tag{44d}$$

$$A'_1=-\omega^6\tau_F^4\tau^2+\omega^4\tau_F^2\tau^2\left[13+\frac{11}{3}\frac{\tau_F}{\tau}\right]-\omega^2\tau_F^2\left[\frac{85}{36}+\frac{46}{3}\frac{\tau}{\tau_F}+4\frac{\tau^2}{\tau_F^2}\right]+\frac{4}{3}\ , \tag{44e}$$

$$B'_1=6\omega^4\tau_F^3\tau-\omega^2\tau_F\tau\left[12+\frac{41}{3}\frac{\tau_F}{\tau}\right]+\frac{2}{3}\left[8+\frac{16}{3}\frac{\tau_F}{\tau}\right]\ . \tag{44f}$$

If in Eqs. (43a)–(43d) we let τ_F tend to zero, the well-known noninertial harmonic components are recovered [11].

It is also interesting to write down in normalized form the time-independent component of the birefringence in terms of τ_F, τ, and P, in order to compare it with that which we have previously derived for zero inertia [11]. Thus we obtain

$$\langle P_2\rangle_{\rm st}^N(\omega)=\frac{\langle P_2\rangle_{\rm st}(\omega)}{\langle P_2\rangle_{\rm st}(0)}$$

$$=\frac{1}{P+1}\left[P+\frac{1}{1+\frac{2E_c^2}{E_0^2}}\left[2\frac{E_c^2}{E_0^2}+\frac{1}{6}\frac{\omega^4\tau_F^3\tau+4\omega^2\tau\tau_F\left[1+\frac{7}{6}\frac{\tau_F}{\tau}\right]+\frac{8}{3}}{\left[-3\omega^2\tau_F\tau+\frac{2}{3}\right]^2+\omega^2\tau_F^2\left[-\omega^2\tau_F\tau+2\frac{\tau}{\tau_F}+\frac{5}{6}\right]^2}\right]\right]\ , \tag{45}$$

where the superscript N stands for normalized. As $I\to 0$ or $\tau_F\to 0$, we find that

$$\lim_{\tau_F\to 0}\langle P_2\rangle_{\rm st}^N(\omega)$$

$$=\frac{1}{P+1}\left[P+\frac{1}{1+\frac{2E_c^2}{E_0^2}}\left[2\frac{E_c^2}{E_0^2}+\frac{1}{1+\left[\frac{\omega}{2D}\right]^2}\right]\right]\ , \tag{46}$$

where D is the rotational diffusion coefficient defined by Einstein's relation

$$D=\frac{kT}{\xi}=\frac{1}{6\tau}\ . \tag{47}$$

Equation (46) agrees fully with our Eq. (5) of Ref. [11]. In the case of purely polar molecules ($P\to\infty$) under the influence of a pure ac field ($E_c=0$), Eq. (45) reduces to the sole frequency-dependent part that never becomes negative, as can be seen from the denominator of this equation (imaginary roots only). This result is in agreement with an early work of Rocard [16]. This remark is important to confirm the validity of the truncation at $n=3$ of the transition matrix where it is also meant that only small inertial effects are taken into account. In order to see their importance on the general behavior of the Kerr effect response, it is convenient to introduce the dimensionless inertial parameter γ defined by

$$\gamma=\frac{\beta^2}{\alpha^2}=\frac{\xi^2}{IkT}=\frac{1}{6}\frac{\tau_F}{\tau}\ . \tag{48}$$

This relation shows that γ measures the balance between τ_F and τ. Following Sack [17], convergence of the nonlinear terms in the 3×3 approximation is ensured provided $\gamma<0.0167$. Another physical quantity merits some attention, namely, the phase angle $\theta_j(\omega)$ existing between in-phase and out-of-phase birefringence harmonic components and characterizing the dispersive nature of the dielectric liquid submitted to an ac electric field. We obviously have

$$\theta_j(\omega)=\tan^{-1}\frac{Y_j(\omega)}{X_j(\omega)}\ . \tag{49}$$

This equation must be used carefully insofar as the inverse circular function ($\tan^{-1}$) is a multiform function having an infinite number of determinations. Within the range $0<\omega<+\infty$, the phase angle is continuous so that the principal determination $(\tan^{-1})_{\rm P}$, denoted by the subscript P, is not always valid. We then have

$$(\tan^{-1})=(\tan^{-1})_{\rm P}+k_1\pi\ , \tag{50}$$

where k_1 is an integer. This last comment applies particularly to computer users where the principal determination $(\tan^{-1})_P$ is systematically employed and may lead to erroneous calculations.

VI. NUMERICAL ANALYSIS OF THE 3×3 APPROXIMATION FOR THE SYMMETRIC TOP MODEL

We shall first examine the plots of X_j and Y_j against ω (dispersion and absorption spectra) for various values of P and a fixed value of $\gamma=0.016$. The cases $P<-1$ and $P>-1$ are well differentiated for both harmonic components because the normalization factor is proportional to $P+1$. All these curves present a resonant behavior that manifests itself by the existence of a common intersection point, which is independent of P, and is not apparent at all for the $Y_j(\omega)$ plots with zero inertia. It is instructive to note that the real parts $X_j(\omega)$ also have such a common point regardless of γ. We have verified that the frequency related to these points is monotonically decreasing as γ increases. Moreover, the peaks of $Y_j(\omega)$ are shifted toward the right of the frequency domain as P lies between $-\infty$ and $+\infty$, with increasing amplitudes for $-\infty<P<-1$ and decreasing ones for $-1<P<+\infty$. For both harmonic components, we see the appearance of overshoots for the $X_j(\omega)$ plots ($X_j>1$) in the interval $-\frac{5}{2}\leq P<-1$. All these considerations are illustrated in Figs. 2–5.

We shall now study the Cole-Cole diagrams, that is, the variations of Y_j against X_j. We have chosen the same P values as those used in our previous paper [11] in order to compare the results with each other. For $P<-1$, it is shown that X_j may take negative values, which is not the case at zero inertia. So the relevant plots are deformed in the high-frequency region with ends tending tangentially to the OX_j axis instead of the OY_j axis (Figs. 6 and 7). For $-1<P<+\infty$, the situation becomes a little more intricate. One may, however, overcome this difficulty by considering some interesting limiting P values. These are $P=-\frac{1}{2}$ for the first harmonic component ($H1$) and $P=0$ for the second one ($H2$), which correspond to highly polar molecules ($\Delta\alpha=0$), as can be seen from Eqs. (43a)–(43d). Regarding $H2$ in the range $-1<P\leq 0$, we see that the solution of $X_2(\omega)=0$ consists of two zeros instead of only one at zero inertia, so that the high-frequency part of $Y_2(X_2)$ tends to the OX_2 axis (Fig. 8). The same trend is observed for $H1$ in the range $-1<P\leq -1/2$ (Fig. 9). As P becomes positive for $H2$ or greater than $-\frac{1}{2}$ for $H1$, the role of molecular inertia is characterized by negative values of $X_j(\omega)$ at highest frequencies. This is not observed in the rotational diffusion limit ($I\rightarrow 0$, ξ being finite). Generally speaking, all these curves show similarities to the corresponding curves of the noninertial response in the very low frequency region; however, they deviate considerably for increasing values of γ and ω, then exhibiting skewed arcs (deformed quasiconchoids of circles).

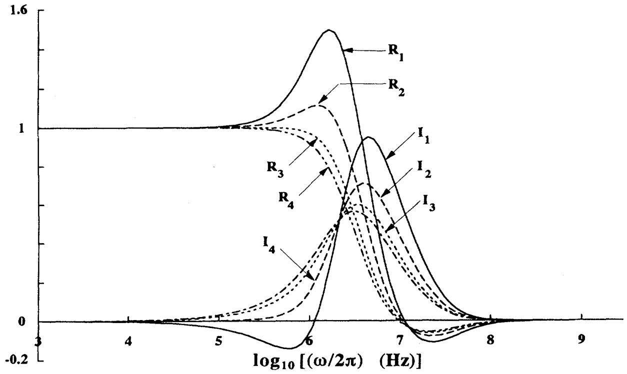

FIG. 2. Dispersion and absorption plots of the second harmonic component of the birefringence for $P<-1$ and $\gamma=0.016$. R and I stand for the real and imaginary parts of the complex birefringence. The subscripts 1–4 denote various P values. 1, $P=-1.7$; 2, $P=\frac{5}{2}$; 3, $P=-\frac{19}{4}$ 4, $P=-10$.

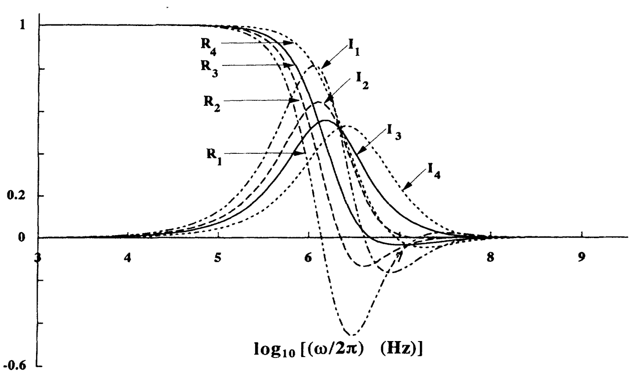

FIG. 3. Same as Fig. 2 for $P>-1$. 1, $P=-0.4$; 2, $P=0$; 3, $P=\frac{2}{3}$; 4, $P=10$.

We may complete this description by considering molecules having induced dipole moments only ($\mu=0$), so that $P\rightarrow\pm\infty$ ($\Delta\alpha>0$ or <0). In practice, the prevalence of the electric polarizabilities over the permanent moments is sufficiently fulfilled for $|P|>10$, say. The right-hand sides of Eqs. (43a) and (43c) then reduce to the second term of the sum in the large square brackets. If we solve $X_j(\omega)=0$, namely,

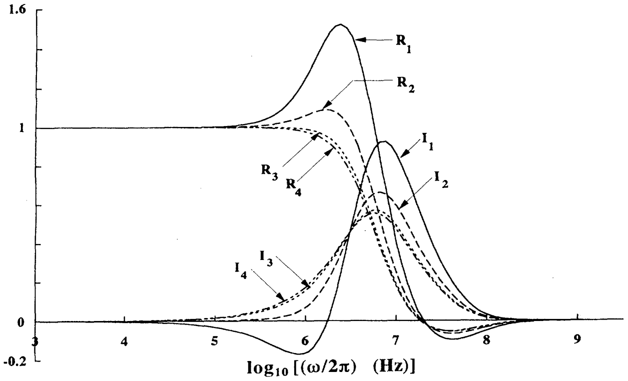

FIG. 4. Dispersion and absorption plots of the first harmonic component of the birefringence for $P<-1$ and $\gamma=0.016$. 1, $P=-1.5$; 2, $P=-\frac{5}{2}$; 3, $P=-7$; 4, $P=-15$.

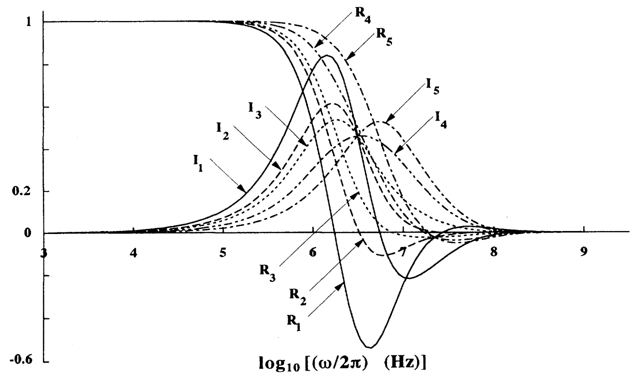

FIG. 5. Same as Fig. 4 for $P>-1$. 1, $P=-0.7$; 2, $P=-0.5$; 3, $P=-\frac{1}{3}$; 4, $P=\frac{1}{2}$; 5, $P=10$.

$$-24\omega^4\tau_F^3\tau-\omega^2\tau_F\tau\left[-4+17\frac{\tau_F}{\tau}\right]+6=0 \qquad \text{for } j=2\ (H2) \qquad (51a)$$

and

$$-\omega^4\tau_F^3\tau-\omega^2\tau_F\tau\left[-4+\frac{17}{6}\frac{\tau_F}{\tau}\right]+4=0 \qquad \text{for } j=1\ (H1)\ , \qquad (51b)$$

we find that these two equations have the same real solution for small γ values,

$$\omega^2\approx\frac{1}{4\tau_F\tau} \quad \text{or} \quad \omega^2\approx\frac{3}{2}\frac{kT}{I}\ . \qquad (51c)$$

This result shows that the angular velocity for which the real part of the birefringence is zero lies in the high-frequency domain. As $I\rightarrow 0$, we can verify that the plots $Y_j(X_j)$ have no intersection points with the OY_j axis and tend tangentially to this axis. Hence Eq. (51c) allows us to extract the moment of inertia of the highly anisotropic molecule, $I\approx 3kT/(2\omega^2)$. Indeed, it is always possible by experiment to determine the absolute temperature T together with the angular frequency ω for which $X_j(\omega)=0$.

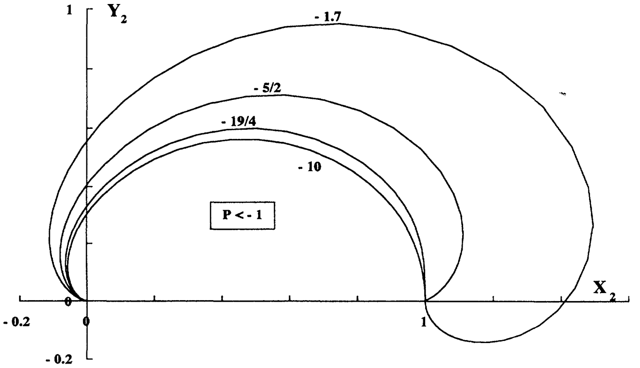

FIG. 6. Cole-Cole plots of the second harmonic component of the birefringence for $P<-1$ and $\gamma=0.016$. The numbers above or below the plots are for various P values.

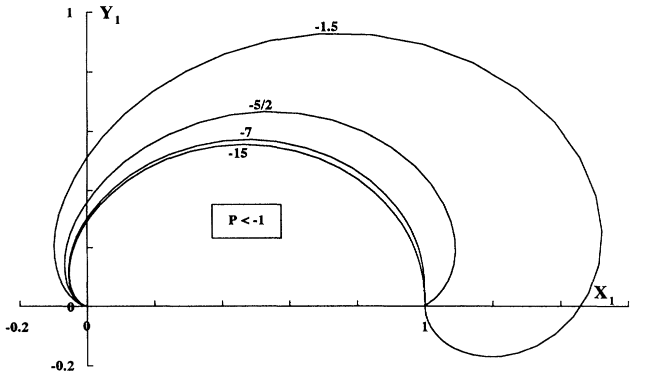

FIG. 7. Cole-Cole plots of the first harmonic component of the birefringence for $P<-1$ and $\gamma=0.016$. The numbers above or below the plots are for various P values.

For other values of P, the analytic solution of $X_j(\omega)=0$ or $Y_j(\omega)=0$ does not provide simple expressions for ω. They may be found, however, by numerical methods. Moreover, the angular frequencies corresponding to $X_j(\omega)=0$ or $Y_j(\omega)=0$ may always be determined experimentally. Thus the best-fit procedure is a suitable technique to obtain the relaxation times τ_F and τ. The moment of inertia is therefore simply given by $I=6kT\tau_F\tau$. In the low-frequency region, inertial effects are unimportant so that a good estimate of P and τ may be made by using our previous results detailed in Ref. [11].

The general features of the Cole-Cole plots in the high-frequency region entail deep modifications of the variations of the phase angles in this region. We shall focus on this aspect in the next section.

VII. STUDY OF THE PLOTS $\theta_j(\omega)$

For high values of ω, the amplitude of the birefringence response is very small and may be the cause of inaccurate data if the signal-to-noise ratio is bad. This difficulty may be overcome if one notes (from the Cole-Cole plots) that the variations of $\theta_j(\omega)$ as ω becomes large can be multiplied up to a factor 2 compared to

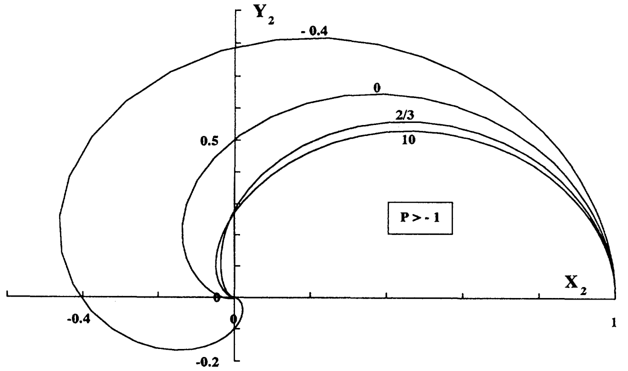

FIG. 8. Same as Fig. 6 for $P>-1$.

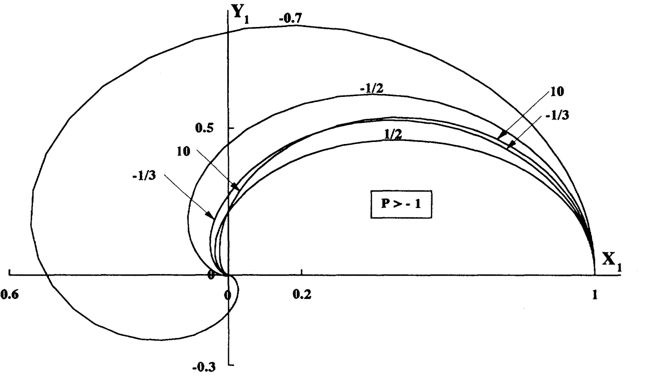

FIG. 9. Same as Fig. 7 for $P > -1$.

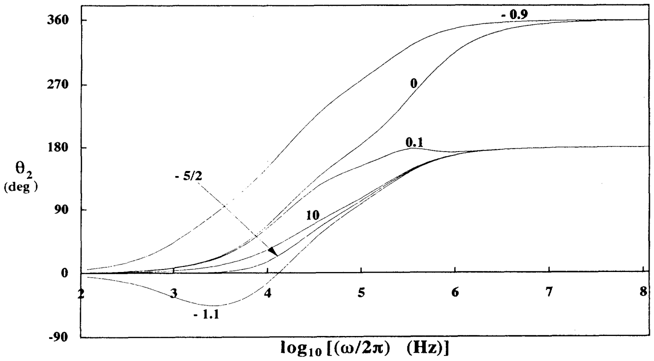

FIG. 10. Plots of the phase angles versus $\log_{10}(\omega/2\pi)$ for the second harmonic component of the birefringence. The numbers above or below the plots are for various P values.

those obtained for $\gamma=0$, thus allowing a possible practical application with increased precision.

We shall examine the plots of $\theta_j(\omega)$ as functions of ω for various values of P and $\gamma=0.016$ (Figs. 10 and 11). We first concentrate on the limiting values of P, $P=\pm\infty$, corresponding to nonpolar molecules. The asymptotic value attained by $\theta_j(\omega)$ goes from $\pi/2$ for $\gamma=0$ to π for $\gamma=0.016$. In the case of polar molecules only, $P=0$ ($H2$) or $P=-\frac{1}{2}$ ($H1$), we note also the doubling of the phase angle in the limit of high frequencies. Close to these values, $P=0.1$ ($H2$) or $P=-0.49$ ($H1$), we see that $\theta_j(\omega)$ presents a maximum that exceeds slightly π and then tends to π, exhibiting a value twice that obtained for $\gamma=0.1$. Near $P=-1$, the plots are completely different according to $P=-1^+$ or $P=-1^-$. For $P=-0.9$, $\theta_j(\infty)=2\pi$ when $\gamma=0.016$, whereas $\theta_j(\infty)=3\pi/2$ when $\gamma=0$: here the multiplicative factor is $\frac{4}{3}$. For $P=-1.1$, $\theta_j(\omega)$ passes through a minimum (negative value) and tends to π when $\gamma=0.016$ instead of $\pi/2$ when $\gamma=0$.

In conclusion, our investigation on the phase angles between the real and imaginary parts of the complex birefringence functions leads, when molecular inertia is included, to values that deviate very clearly from those obtained at zero inertia in proportion to increasing frequencies. Moreover, use of coupled fields allows us to work with a double set of information on parameters such as P, τ_F, and τ since it is always possible to measure separately the first and the second harmonic components.

APPENDIX A

Here we shall calculate the transition matrix $[\mathbf{M}_2]$ up to the 5×5 approximation in order to see how the set of differential equations characteristic of the Kerr-effect relaxation is constructed. From Eq. (6), we have

$$\dot{\Omega}_1=-\alpha\sqrt{2}\Omega_2\Omega_3+\alpha\sqrt{2}\Omega_2^2\cot\vartheta-\beta\Omega_1 -\frac{\mu E}{I\alpha\sqrt{2}}\sin\vartheta-\frac{\Delta\alpha}{I\alpha\sqrt{2}}E^2\sin\vartheta\cos\vartheta+\frac{\lambda_1}{I\alpha\sqrt{2}},$$
$$\dot{\Omega}_2=\alpha\sqrt{2}\Omega_1\Omega_3-\alpha\sqrt{2}\Omega_1\Omega_2\cot\vartheta-\beta\Omega_2+\frac{\lambda_2}{I\alpha\sqrt{2}}, \tag{A1}$$
$$\dot{\Omega}_3=-\beta\Omega_3+\frac{\lambda_3}{I\alpha\sqrt{2}}.$$

In view of deriving Eq. (22), it is also convenient to know the general expressions for symmetric tops of the time derivatives of the Hermite polynomials, namely,

$$\langle\dot{H}_n(\Omega_1)\rangle=-\frac{\alpha\sqrt{2}}{2}n\langle H_{n-1}(\Omega_1)H_1(\Omega_2)H_1(\Omega_3)\rangle+\frac{\alpha\sqrt{2}}{2}n\langle H_{n-1}(\Omega_1)[H_2(\Omega_2)+2]\cot\vartheta\rangle$$
$$-n\beta\langle H_n(\Omega_1)\rangle-2n\frac{\mu}{I\alpha\sqrt{2}}\langle H_{n-1}(\Omega_1)E\sin\vartheta\rangle-2n\frac{\Delta\alpha}{I\alpha\sqrt{2}}\langle H_{n-1}(\Omega_1)E^2\sin\vartheta\cos\vartheta\rangle, \tag{A2}$$

$$\langle\dot{H}_n(\Omega_2)\rangle=\frac{\alpha\sqrt{2}}{2}n\langle H_1(\Omega_1)H_{n-1}(\Omega_2)H_1(\Omega_3)\rangle$$
$$-\frac{\alpha\sqrt{2}}{2}n\langle H_1(\Omega_1)[H_n(\Omega_2)+2(n-1)H_{n-2}(\Omega_2)]\cot\vartheta\rangle-n\beta\langle H_n(\Omega_2)\rangle, \tag{A3}$$

$$\langle\dot{H}_n(\Omega_3)=-n\beta\langle H_n(\Omega_3)\rangle, \tag{A4}$$

$$\frac{d}{dt}\langle[H_{n-p}(\Omega_2)H_p(\Omega_3)]\rangle=-p\beta\langle H_{n-p}(\Omega_2)H_p(\Omega_3)\rangle+(n-p)\frac{\alpha\sqrt{2}}{2}\langle H_1(\Omega_1)H_{n-p-1}(\Omega_2)H_1(\Omega_3)H_p(\Omega_3)\rangle$$
$$-(n-p)\frac{\alpha\sqrt{2}}{2}\langle H_1(\Omega_1)[H_{n-p}(\Omega_2)+2(n-p-1)H_{n-p-2}(\Omega_2)]\cot\vartheta H_p(\Omega_3)\rangle$$
$$-(n-p)\beta\langle H_{n-p}(\Omega_2)H_p(\Omega_3)\rangle. \tag{A5}$$

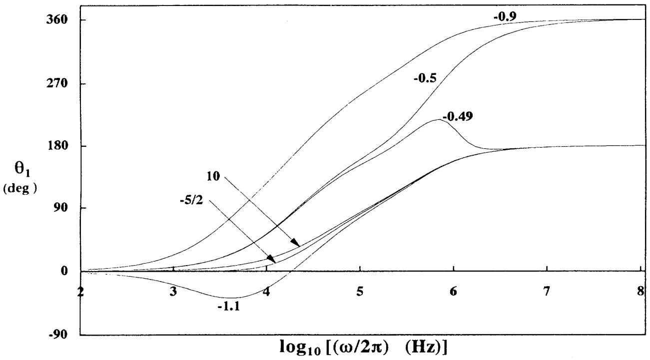

FIG. 11. Same as Fig. 10 for the first harmonic component of the birefringence.

From these equations and noting that

$$P_2^1\cot\vartheta=2P_2+1\ ,\quad \dot{P}_2^1=\frac{\alpha\sqrt{2}}{2}(4P_2-1)H_1(\Omega_1)\ ,$$
$$(P_2-1)\cot\vartheta=-\tfrac{1}{2}P_2^1\ , \tag{A6}$$

Eq. (23) may be readily found.

The same method may be applied to carry out $\langle\dot{Z}_3\rangle$ from Eq. (25b). Insofar as we wish to prove that matrix truncations of the form 3×3 and 4×4 give similar results, it is sufficient here to consider the step-off solution, which allows us to simplify the literal expressions without obscuring the physics of our problem. This leads to

$$\langle\dot{Z}_3\rangle=-3\beta\langle Z_3\rangle+\alpha\sqrt{2}\langle Z_4\rangle+7\alpha\sqrt{2}\langle Z_2\rangle+\frac{3\alpha}{\sqrt{2}}\langle Z_2'\rangle\ , \tag{A7}$$

where $\langle Z_4\rangle$ contains Hermite polynomials of fourth order and

$$\langle Z_2'\rangle=\langle P_2[H_2(\Omega_1)+H_2(\Omega_2)+H_2(\Omega_3)]\rangle\ , \tag{A8}$$

is a term formed of second-order Hermite polynomials such as $\langle Z_2\rangle$. Hence the hierarchy of differential equations in the 4×4 approximation is

$$\begin{bmatrix}\langle\dot{P}_2\rangle\\ \langle\dot{Z}_1\rangle\\ \langle\dot{Z}_2\rangle\\ \langle\dot{Z}_2'\rangle\end{bmatrix}=\begin{bmatrix}0 & -\dfrac{\alpha\sqrt{2}}{2} & 0 & 0\\ 6\alpha\sqrt{2} & -\beta & \alpha\sqrt{2} & 0\\ 0 & -\dfrac{11\alpha\sqrt{2}}{2} & -2\beta & 0\\ 0 & -2\alpha\sqrt{2} & 0 & -2\beta\end{bmatrix}\begin{bmatrix}\langle P_2\rangle\\ \langle Z_1\rangle\\ \langle Z_2\rangle\\ \langle Z_2'\rangle\end{bmatrix}\ , \tag{A9}$$

or in matrix notation

$$[\dot{\mathbf{p}}_2(t)]=[\mathbf{M}_2][\mathbf{p}_2(t)]\ .$$

In order to manipulate normalized expressions, we may take the initial condition

$$\begin{bmatrix}\langle P_2\rangle(0)\\ \langle Z_1\rangle(0)\\ \langle Z_2\rangle(0)\\ \langle Z_2'(0)\rangle\end{bmatrix}=\begin{bmatrix}1\\0\\0\\0\end{bmatrix}\ . \tag{A10}$$

We may therefore calculate the orientational correlation time defined by

$$\tau^{(2)}=\lim_{s\to 0}\int_0^{+\infty}e^{-st}\langle P_2\rangle(t)dt=\lim_{s\to 0}L(\langle P_2\rangle(t))\ , \tag{A11}$$

where L denotes "the Laplace transform of." The solution of Eq. (A9) may be expressed as

$$[\mathbf{p}_2(t)]=L^{-1}\{s[\mathbf{I}]-[\mathbf{M}_2]\}^{-1}\ , \tag{A12}$$

so that the determinants of $\{s[\mathbf{I}]-[\mathbf{M}_2]\}$ in the 3×3 and 4×4 approximations are

$$\det\{s[\mathbf{I}]-[\mathbf{M}_2]\}_{3\times3}=s[(s+\beta)(s+2\beta)+11\alpha^2]+6\alpha^2(s+2\beta)\ , \tag{A13}$$

$$\begin{aligned}\det\{s[\mathbf{I}]-[\mathbf{M}_2]\}_{4\times4}&=(s+2\beta)\{s[(s+\beta)(s+2\beta)+11\alpha^2]+6\alpha^2(s+2\beta)\}\\&=(s+2\beta)\det\{s[\mathbf{I}]-[\mathbf{M}_2]\}_{3\times3}\ ,\end{aligned} \tag{A14}$$

respectively. Thus the Laplace transform of the step-off solution $\langle P_2\rangle(t)$ is

$$L[\langle P_2\rangle(t)]_{n\times n}=\frac{(a_{11})_{n\times n}}{\det\{s[\mathbf{I}]-[\mathbf{M}_2]\}_{n\times n}}\ , \tag{A15}$$

where $(a_{11})_{n\times n}$ is the first element of $\mathrm{adj}\{s[\mathbf{I}]-[\mathbf{M}_2]\}_{n\times n}$. We find that

$$(a_{11})_{3\times3}=(s+\beta)(s+2\beta)+11\alpha^2\ , \tag{A16}$$

$$\begin{aligned}(a_{11})_{4\times4}&=(s+2\beta)[(s+\beta)(s+2\beta)+11\alpha^2]\\&=(s+2\beta)(a_{11})_{3\times3}\ .\end{aligned} \tag{A17}$$

From Eqs. (A13), (A14), (A16), and (A17), it is clear that

$$L[\langle P_2\rangle(t)]_{3\times3}=L[\langle P_2\rangle(t)]_{4\times4}\ , \tag{A18}$$

whence

$$\tau^{(2)}_{3\times3}=\tau^{(2)}_{4\times4}=\frac{2\beta^2+11\alpha^2}{12\alpha^2\beta}=\tau\left[1+\frac{11}{2}\gamma\right]\ , \tag{A19}$$

with $\tau=\xi/(6kT)=\beta/(6\alpha^2)$.

Thus the next approximation following 3×3 will be 5×5. By inspection of Eq. (A7), the relevant matrix to this is

$$[\mathbf{M}_2]_{5\times5}=\begin{bmatrix} 0 & -\frac{\alpha\sqrt{2}}{2} & 0 & 0 & 0 \\ 6\alpha\sqrt{2} & -\beta & \alpha\sqrt{2} & 0 & 0 \\ 0 & -\frac{11\alpha\sqrt{2}}{2} & -2\beta & 0 & -\alpha\sqrt{2} \\ 0 & -2\alpha\sqrt{2} & 0 & -2\beta & -\frac{\alpha\sqrt{2}}{2} \\ 0 & 0 & 7\alpha\sqrt{2} & \frac{3\alpha\sqrt{2}}{2} & -3\beta \end{bmatrix}, \tag{A20}$$

from which we have

$$\begin{aligned}\det\{s[\mathbf{I}]-[\mathbf{M}_2]\}_{5\times5} &\\ =s\{&(s+\beta)(s+2\beta)[(s+2\beta)(s+3\beta)+\tfrac{31}{2}\alpha^2] \\ &+11\alpha^2(s+2\beta)(s+3\beta)+\tfrac{9}{2}\alpha^4\} \\ &+6\alpha^2(s+2\beta)[(s+2\beta)(s+3\beta)+\tfrac{31}{2}\alpha^2]\ ,\end{aligned} \tag{A21}$$

$$\begin{aligned}(a_{11})_{5\times5}=&(s+\beta)(s+2\beta)[(s+2\beta)(s+3\beta)+\tfrac{31}{2}\alpha^2] \\ &+11\alpha^2(s+2\beta)(s+3\beta)+\tfrac{9}{2}\alpha^4\ ,\end{aligned} \tag{A22}$$

whence

$$\tau^{(2)}_{5\times5}=\frac{12\beta^4+97\alpha^2\beta^2+\frac{9}{2}\alpha^4}{6\alpha^2\beta(12\beta^2+31\alpha^2)}=\tau\left[1+\frac{11}{2}\gamma-\frac{83}{6}\gamma^2\right]. \tag{A23}$$

Equations (A19) and (A23) agree with those obtained by McConnell [1] who used stochastic rotation operators, allowing one to calculate the normalized autocorrelation function of the spherical harmonic $Y_{2m}(\vartheta(t),\varphi(t))$ appropriate to $l=2$ processes.

APPENDIX B

In the derivation of Eq. (19b) giving the time evolution of the second Legendre polynomial, we have started from the first Euler-Langevin equation [Eq. (6a)] in which we have changed the variable ϑ into $P_2(\cos\theta)$. We think it interesting to obtain a more general formulation concerning the time evolution of the nth Legendre polynomial. This would be useful to carry out higher-order nonlinear responses (greater than 2).

As currently done, we set as variable $u=\cos\vartheta$, so that

$$\dot u=-\dot\vartheta\sin\vartheta=-(1-u^2)^{1/2}\dot\vartheta\ , \tag{B1}$$

$$\ddot u=-(\dot\vartheta^2\cos\vartheta+\ddot\vartheta\sin\vartheta)=-[u\dot\vartheta^2+(1-u^2)^{1/2}\ddot\vartheta]\ . \tag{B2}$$

Now, if the new variable in Eq. (6a) is $P_n(\cos\vartheta)=P_n(u)$, we must evaluate

$$\dot P_n(u)=\frac{dP_n}{du}\frac{du}{dt}=-(1-u^2)^{1/2}\dot\vartheta\frac{dP_n}{du}\ , \tag{B3}$$

$$\begin{aligned}\ddot P_n(u)&=\dot u^2\frac{d^2P_n}{du^2}+\ddot u\frac{dP_n}{du} \\ &=(1-u^2)\dot\vartheta^2\frac{d^2P_n}{du^2}-[u\dot\vartheta^2+(1-u^2)^{1/2}\ddot\vartheta]\frac{dP_n}{du}\ .\end{aligned} \tag{B4}$$

From Eq. (B4), we have

$$\dot\omega_1(t)=\ddot\vartheta(t)=-\frac{\ddot P_n-[(1-u^2)P_n''-uP_n']\dot\vartheta^2}{(1-u^2)^{1/2}P_n'}\ , \tag{B5}$$

where

$$P_n'=\frac{dP_n}{du}\ ,\quad P_n''(u)=\frac{d^2P_n}{du^2}\ .$$

Using the recursion formulas

$$(1-u^2)P_n''=2uP_n'-n(n+1)P_n\ ,$$

$$(1-u^2)P_n'=n(P_{n-1}-uP_n)\ ,$$

$$(2n+1)uP_n=(n+1)P_{n+1}+nP_{n-1}\ ,$$

Eq. (B5) becomes

$$\begin{aligned}\ddot\vartheta(t)&=-\frac{\ddot P_n-[uP_n'-n(n+1)P_n]\dot\vartheta^2}{(1-u^2)^{1/2}P_n'} \\ &=-\frac{\ddot P_n+\left[\frac{n(n-1)}{2n-1}(P_n-P_{n-2})\frac{1}{1-u^2}+n^2P_n\right]\dot\vartheta^2}{(1-u^2)^{-1/2}n(P_{n-1}-uP_n)} \\ &=-\frac{\ddot P_n+\left[\frac{n(n-1)}{2n-1}(P_n-P_{n-2})\frac{1}{1-u^2}+n^2P_n\right]\dot\vartheta^2}{(1-u^2)^{-1/2}\frac{n(n+1)}{2n+1}(P_{n-1}-P_{n+1})}\ .\end{aligned} \tag{B6}$$

Substituting Eq. (B6) into Eq. (6a) yields

$$
\begin{aligned}
&I\ddot{P}_n+I\left[\frac{1}{1-u^2}\frac{n(n-1)}{2n-1}(P_n-P_{n-2})+n^2P_n\right]\dot{\vartheta}^2\\
&\quad+I\left\{\frac{1}{1-u^2}\left[\frac{n(n+1)}{(2n-1)(2n+3)}P_n+\frac{(n-1)n(n+1)}{(2n-1)(2n+1)}P_{n-2}-\frac{n(n+1)(n+2)}{(2n+1)(2n+3)}P_{n+2}\right]\right\}\omega_2^2\\
&\quad+\xi\dot{P}_n-I\omega_2\omega_3(1-u^2)^{-1/2}\frac{n(n+1)}{2n+1}(P_{n-1}-P_{n+1})\\
&\quad=\mu E(t)\frac{n(n+1)}{2n+1}(P_{n-1}-P_{n+1})\\
&\qquad+\Delta\alpha E^2(t)\left[\frac{n(n+1)}{(2n-1)(2n+3)}P_n+\frac{(n-1)n(n+1)}{(2n-1)(2n+1)}P_{n-2}-\frac{n(n+1)(n+2)}{(2n+1)(2n+3)}P_{n+2}\right]\\
&\qquad-\lambda_1(1-u^2)^{-1/2}\frac{n(n+1)}{2n+1}(P_{n-1}-P_{n+1})\;. \qquad \text{(B7)}
\end{aligned}
$$

In particular, Eq. (27a) may be found by setting $n=1$ in Eq. (B7). Also, the infinite hierarchy of differential-recurrence relations may be directly established from this equation as $I\rightarrow 0$. In this case, the ensemble averages of the last terms on the left- and right-hand sides of Eq. (B7) are zero, so that Eq. (B7) reduces exactly to Eq. (17).

[1] J. R. McConnell, *Rotational Brownian Motion and Dielectric Theory* (Academic, London, 1980).

[2] W. T. Coffey, J. Chem. Phys. **95**, 2026 (1991).

[3] W. T. Coffey, Chem. Phys. **143**, 171 (1990).

[4] J. L. Déjardin, J. Chem. Phys. **95**, 576 (1991).

[5] J. L. Déjardin and G. Debiais, J. Chem. Phys. **95**, 2787 (1991).

[6] Y. P. Kalmykov and K. P. Quinn, J. Chem. Phys. **95**, 9142 (1991).

[7] W. T. Coffey, J. L. Déjardin, Y. P. Kalmykov, and K. P Quinn, Chem. Phys. **164**, 357 (1992).

[8] W. T. Coffey, P. J. Cregg, and Y. P. Kalmykov, in *On the Theory of Debye and Néel Relaxation of Single Domain Ferromagnetic Particles,* edited by I. Prigogine and S. A. Rice, Advances in Chemical Physics Vol. 83 (Wiley-Interscience, New York, 1992), p. 263.

[9] P. Debye, *Polar Molecules* (Chemical Catalog, New York, 1929).

[10] W. T. Lotschaw, D. McMorrow, C. Kalpouzos, and G. A. Kenney-Wallace, Chem. Phys. Lett. **136**, 323 (1987).

[11] J. L. Déjardin and G. Debiais, Phys. Rev. A **40**, 1560 (1989).

[12] D. G. Frood and P. Lal (unpublished).

[13] W. T. Coffey, J. Chem. Phys. **99**, 3014 (1993).

[14] H. Risken, *The Fokker-Planck Equation* (Springer-Verlag, Berlin, 1984).

[15] J. L. Déjardin, Doctorat ès-sciences thèse d'Etat, University of Montpellier, Montpellier, France, 1977 (unpublished).

[16] M. Y. Rocard, J. Phys. Radium **4**, 247 (1933).

[17] R. A. Sack Proc. Phys. Soc. London Sect. B **70**, 414 (1957).